 doi:10.20944/preprints202110.0406.v1

Article

Multi stimuli responsive materials supported by orthogonal hydrogen and halogen bonding or I···alkene interaction

Pierre Frangville,[1] Shiv Kumar,[1] Michel Gelbcke,[1] Kristof Van Hecke,[2] and Franck Meyer [1,*]

[1] Microbiology, Bioorganic and Macromolecular Chemistry, Faculty of Pharmacy, Boulevard du Triomphe, 1050 Brussels, Belgium; franck.meyer@ulb.be
[2] XStruct, Department of Chemistry, Ghent University, Krijgslaan 281-S3, B-9000 Ghent, Belgium; kristof.vanhecke@ugent.be
* Correspondence: franck.meyer@ulb.be; Tel.: +32 (0)2 650 51 96

Abstract: Smart materials represent an elegant class of (macro)-molecules endowed with the ability to react to chemical/physical changes in the environment. Herein, we prepared new photo responsive azobenzenes possessing halogen bond donor groups. The X-ray structures of two molecules highlight supramolecular organizations governed by unusual noncovalent bonds. In azo dye **I-azo-NO2**, the nitro group is engaged in orthogonal H···O···I halogen and hydrogen bonding, linking the units in parallel undulating chains. As concern parent **I-azo-NH-MMA**, a non-centrosymmetric pattern is formed due to a very rare I···π interaction involving the alkene group supplemented by hydrogen bonds. The Cambridge Structural Database contains only four structures with the same I···CH_2=C contact. For all compounds, a ^{19}F NMR spectroscopic analysis confirms the formation of halogen bonds in solution through a recognition process with chloride anion, and the reversible photo-responsiveness is demonstrated upon exposing a solution to UV light irradiation. Finally, intermediate **I-azo-NO2** also shows a pronounced color change due to pH variation. These azobenzenes are thereby attractive building blocks to design multi-stimuli responsive materials for highly functional devices.

Keywords: halogen bonding; azobenzene; pH sensitive; stimuli responsive; orthogonal interaction

1. Introduction

Stimuli responsive materials are fascinating compounds with the ability to translate a stimulus into a change of physical/chemical properties at the nano/macro-scale.[1] The careful design of smart systems has opened new perspectives for the conception of next generation of highly functional materials in various domains.[2][3] The chemical toolbox is thereby comprised of a large array of molecular groups that can be finely modified/adapted for the creation of stimuli responsive drug delivery systems, sensors, smart surfaces or purification devices. [4][5] Typically, the responsivity of these compounds is triggered by varied stimuli such as a change of temperature,[6] pH,[7] magnetic environment,[8] redox condition,[9], photo-irradiation[10] and many others. In the arena of smart systems, photo-responsive materials have a photo switching ability in a reversible or irreversible fashion that consists in chemical bond breaking/formation or a conformational change upon irradiation.[11] Among these switchable compounds, azobenzenes represent a very appealing class of molecules that can isomerize from *trans* to *cis* form reversibly.[12] An interesting feature lies in the fact that several synthetic pathways have been developed to prepare symmetric or asymmetric azobenzene derivatives.[13] Moreover, structural modifications of the azobenzene core allow for a fine tuning/shifting of absorbance in the red region and even the near-infrared, whereas shorter wavelength UV radiation is generally used to induce the isomerization.[14][15]

In the last two decades, the halogen bonds (XB), i.e. the interaction involving halogen as acceptor of electronic density, have become of huge interest in the scientific community.[16][17] Although similar in many aspects to the hydrogen bonds, XB have

Preprints (www.preprints.org) | NOT PEER-REVIEWED | Posted: 27 October 2021 doi:10.20944/preprints202110.0406.v1

demonstrated some specificities in synthetic chemistry,[18] biological and materials sciences. [19][20] As far as the applications of azobenzene-based XB donors are concerned, the light induced surface patterning was achieved using asymmetric self-complementary azo dyes linked to poly(4-vinylpyridine) through N···I halogen bonds.[21][22] Other works have reported the formation of photomechanical azo crystals and a gelator capable of undergoing a gel-to-sol transition upon green light irradiation, involving symmetric XB compounds.[23][24] However, only a handful of instance has studied the design and application of such XB molecules, which are usually prepared in moderate yields.[25] Considering this, we decided to develop a straightforward access to photo responsive compounds with XB donor ability. In contrast to azo dyes already described in the literature, these compounds aim at being appended to a substrate such as a polymer which has never been described so far.[26] Recently, we have reported the preparation of multi-responsive polymers having the capability to react to a change of pH, magnetic field and UV-light irradiation.[27] In the same way and as preliminary result to the formation of new XB-based smart materials, our endeavors will be devoted to the synthesis, X-ray structure analysis and determination of physico-chemical properties of new azo dyes endowed with XB donor capability, light responsiveness and even pH sensitivity for a synthetic intermediate.

2. Results & discussion

2.1. Synthesis of halogen bonded azobenzenes

The preparation of halogen bonded azobenzenes was performed through a multistep synthesis (**Figure 1**).

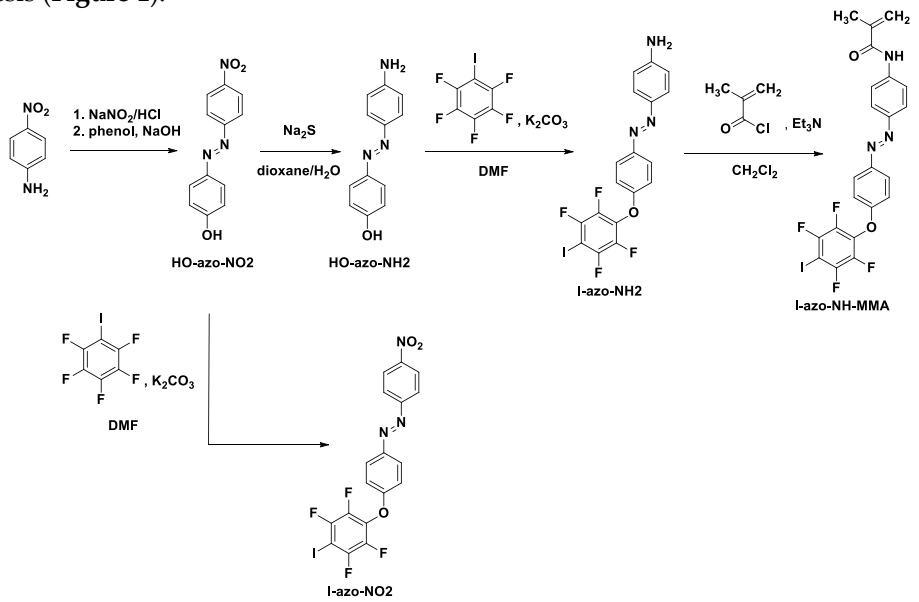

Figure 1. Synthesis of halogen bonded azobenzene derivatives

First of all, the azobenzene core, namely 4-((4-nitrophenyl)diazenyl)phenol (**HO-azo-NO2**), was obtained in 96% yield by diazotization of 4-nitroaniline with sodium nitrite in the presence of hydrochloric acid, followed by coupling reaction with phenol in alkaline conditions, according to a procedure already described in the literature.[28] Subsequently, the incorporation of a halogen bond donor group was operated by nucleophilic replacement of fluorine of pentafluoroiodobenzene using **HO-azo-NO2** and potassium carbonate in dimethylformamide (DMF) at 50 °C. As such, the resulting **I-azo-NO2** was isolated in 95% yield. In order to prepare a polymerizable azobenzene, **HO-azo-NO2** was first reduced with a large excess of sodium sulfide (Na_2S) in a dioxane/water mixture at 90 °C to give **HO-azo-NH2** in 92% yield. Afterwards, the XB donor ring was introduced selectively on hydroxy group to provide **I-azo-NH2** in 91% yield. Finally, **I-azo-NH-MMA** was

Preprints (www.preprints.org) | NOT PEER-REVIEWED | Posted: 27 October 2021 doi:10.20944/preprints202110.0406.v1

obtained by the reaction of methacryloyl chloride and **I-azo-NH2** in the presence of triethylamine in dichloromethane at room temperature in 87% yield.

2.2. X-ray structure analysis of XB azobenzenes

Afterwards, the crystallographic structures of two azobenzene derivatives were studied as first evidence of their ability to form halogen bonds (**Table 1**).

Table 1.X-ray crystal data and refinement parameters for structures **HO-azo-NO2** and **I-azo-NH-MMA**

	HO-azo-NO2	**I-azo-NH-MMA**
Molecular formula	$C_{18}H_8F_4IN_3O_3$	$C_{22}H_{14}F_4IN_3O_2$
Formula weight ($gmol^{-1}$)	517.17	555.26
T (K)	100(2)	100(2)
Crystal system	triclinic	orthorhombic
Space group	P-1 (No. 2)	$Pna2_1$ (No. 33)
a (Å)	5.65780(10)	11.1393(2)
b (Å)	9.9399(2)	5.07170(10)
c (Å)	32.4971(4)	36.6524(7)
α (°)	91.9240(10)	90
β (°)	91.6640(10)	90
γ (°)	105.8040(10)	90
V ($Å^3$)	1756.11(5)	2070.68(7)
Z	4	4
ρ_{calc} (gcm^{-3})	1.956	1.781
μ (mm^{-1})	14.975	12.712
F(000)	1000	1088
$2\theta_{max}$ (°)	147.59	147.34
Measured reflections	61712	7384
Unique reflections	6933	3466
Observed reflections ($I > 2\sigma(I)$)	6250	3128
Parameters refined	523	293
R_1	0.0250	0.0428
wR_2	0.0559	0.1109
R_1 (all data)	0.0302	0.0485
wR_2 (all data)	0.0584	0.1179
Goodness-of-fit (GOF)	1.030	1.054
CCDC-entry	CCDC 2117642	CCDC 2117643

The slow evaporation of a dichloromethane solution of **I-azo-NO2** provided materials with a needle crystal morphology suitable for X-ray diffraction analysis. **I-azo-NO2** crystallized in the centro-symmetric space group P-1, with the asymmetric unit consisting of two complete azobenzene molecules. From a general point of view, the self-complementary azobenzenes develop undulating parallel chains running in opposite directions due to non-covalent bonds (**Figure 2**).

The wavy character of this arrangement is induced by oxygen atoms linking the tetrafluoroiodobenzene group to the azobenzene core, showing dihedral angles of 63.0(1)° and 64.1(1)° between the tetrafluoroiodobenzene and benzene rings, for both molecules, respectively. NO_2···I halogen bonds link the successive molecules into infinite chains and transfer the molecular information between almost equiplanar fluorinated and nitroaryl rings. In details, each iodine interacts with both oxygen atoms of the nitro group, but distances are slightly different, as defined in a Q-type interaction.[29] The I1···O5 and I2···O2 separations are 3.348(2) and 3.308(2) Å, respectively, i.e. around 5% shorter than the sum of van der Waals radii, whereas the I1···O6 and I2···O3 distances are slightly shorter (~90% of the sum of van der Waals radii) (**Table 2**).[30]

Preprints (www.preprints.org) | NOT PEER-REVIEWED | Posted: 27 October 2021 doi:10.20944/preprints202110.0406.v1

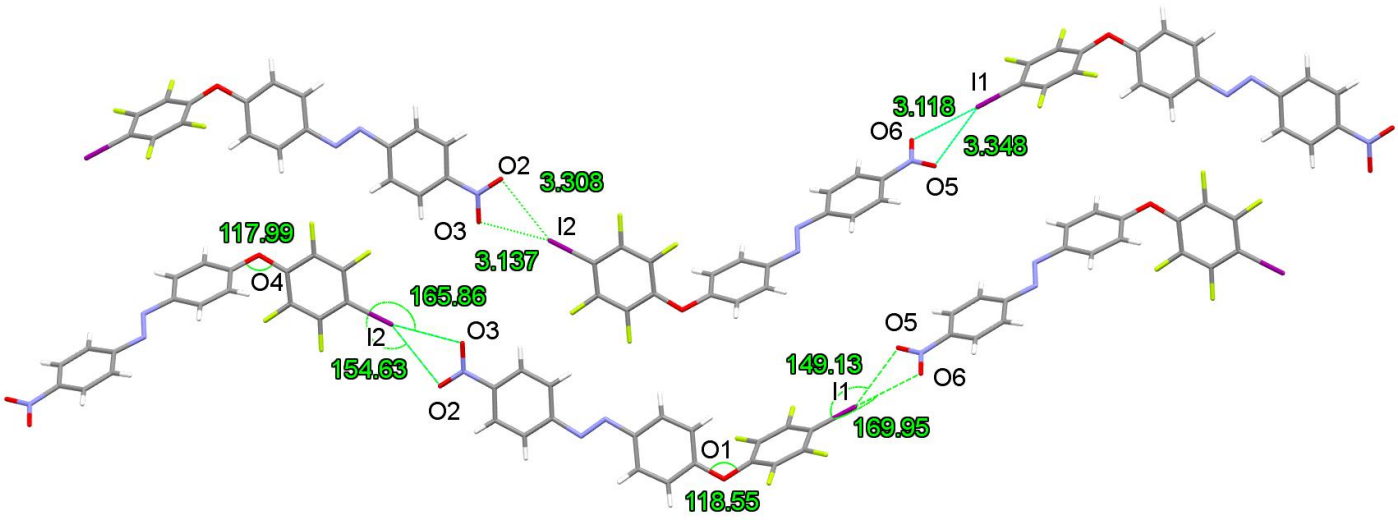

Figure 2. X-ray structure of **I-azo-NO2** developing undulating parallel chains due to two O···I halogen bonds. Colors are as follows: grey, C; blue, N; red, O; white, H; yellow, F; purple, I. O···I bond distances (Å) and C-I···O bond angles (°).

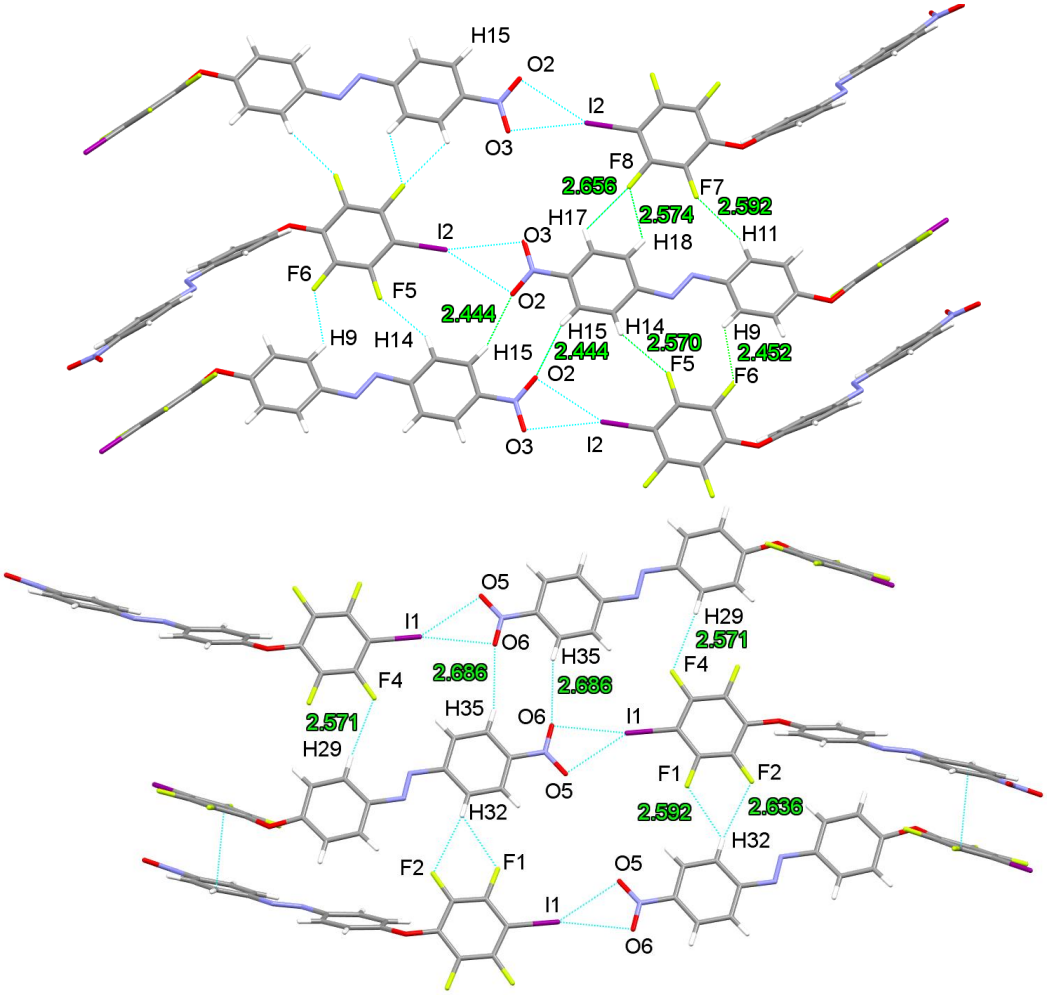

Figure 3. X-ray structure of **I-azo-NO2** highlighting the H15···O2···I2 (top) and H35···O6···I1 (bottom) orthogonal hydrogen and halogen bonds

In all cases, the C-I···O angles are in the range of ~149 to ~170°, which is consistent with halogen bonding parameters. Moreover, two adjacent units pointing in opposite direction are also connected through the nitro group by H15···O2 and H35···O6 hydrogen bonds of

Preprints (www.preprints.org) | NOT PEER-REVIEWED | Posted: 27 October 2021 doi:10.20944/preprints202110.0406.v1

2.444 and 2.686 Å, respectively. Therefore, O2 and O6 are simultaneously engaged in halogen and hydrogen bonds, the H15···O2···I2 and H35···O6···I1 angles being ~100.5 and ~93.7°, respectively (**Figure 3**). To date, few studies have reported an orthogonal relationship between these interactions.[31] Typically, such a supramolecular motif is observed in biological systems with a carbonyl group as electron donor.[32] Recently, a chloride anion was described as hydrogen and halogen bond acceptor in a co-crystal composed of a pyrazolium salt and diiodotetrafluorobenzene.[33] It is interesting to note that the combination of these interactions also occurs in complexes of 4-nitrobenzamide/1,4-diiodobenzene and 1,4-dinitrobenzene/4-iodocinnamic acid.[29][34] Finally, the supramolecular scaffold is stabilized by a myriad of H···F contacts between head-to-tail adjacent molecules (Figure 3 and **Table 2**). The complementary bonded rings (i.e. tetrafluoroiodobenzene group and azobenzene core) belong to the same plane that generates a step-like organization.

Table 2. Parameters of halogen and hydrogen bonds in **I-azo-NO2**

d (I···O), Å	d (I···O)/ΣvdWr, %	< (C-I···O), (H···O···I), °	d (H···O), Å	d (H···F), Å
3.348(2) (I1···O5)	~4.5	149.13 (C-I1···O5)	2.686 (H35···O6)	2.571 (H29···F4)
3.118(2) (I1···O6)	~11	169.95 (C-I1···O6)	2.444 (H15···O2)	2.592 (H32···F1)
3.308(2) (I2···O2)	~5.5	154.63 (C-I2···O2)		2.636 (H32···F2)
3.137(2) (I2···O3)	~10.5	165.86 (C-I2···O3)		2.656 (H17···F8)
		100.54 (H15···O2···I2)		2.574 (H18···F8)
		93.68 (H35···O6···I1)		2.592 (H11···F7)
				2.570 (H14···F5)
				2.452 (H9···F6)

Subsequently, the crystal formation of **I-azo-NH-MMA** was carried out using the aforementioned conditions. The compound crystallized in the non-centrosymmetric space group *P*na2$_1$, with one azobenzene molecule in the asymmetric unit. The X-ray structure of the supramolecular scaffold adopts a similar undulating linear arrangement provoked by tetrahedral geometry of oxygen with sp3 hybridization (**Figure 4**). Here, successive units are linked due to I···π halogen bonds involving the alkene functional group. The crystallographic parameters are in agreement with a halogen bond interaction, namely a I···C22 distance of 3.440(8) Å and a C-I···C22 angle close to linearity (165.1(3)°). Interestingly, the iodine atom makes a perpendicular approach to the double bond (C20-C22···I angle ~90°) emphasizing the electron donation from the p orbital.

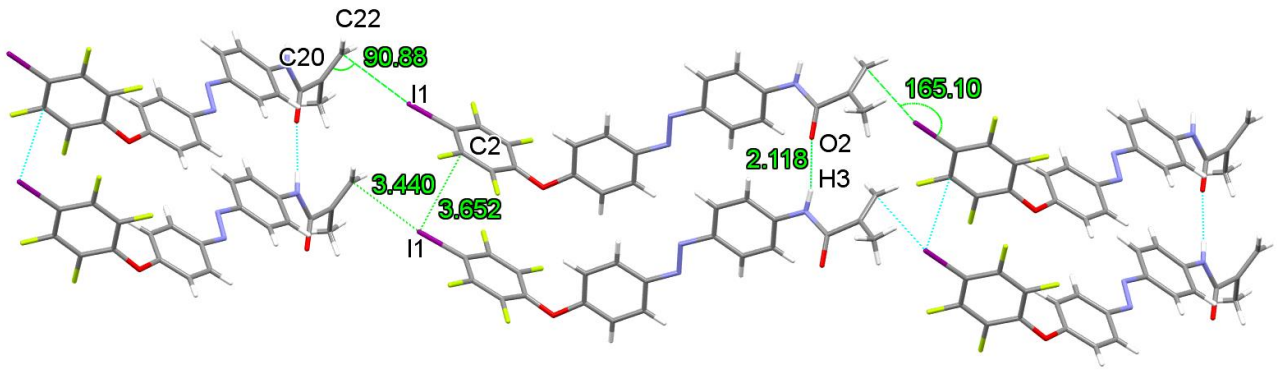

Figure 4. X-ray structure of **I-azo-NH-MMA** developing undulating parallel chains due to C···I halogen bonds

This intriguing contact convinced us to make a Cambridge Structural Database (CSD version 5.42 updates, Sep 2021) analysis on the interaction between an iodine and a double bond (I···CH$_2$=C). This survey reveals that only four molecules adopt the same structural motif, namely HOQKAC,[35] HOTZOH,[36] PEQVOZ[37] and USAJIK.[38] In these X-ray structures, the I···C interactions appear much weaker than in **I-azo-NH-MMA**, since the

Preprints (www.preprints.org) | NOT PEER-REVIEWED | Posted: 27 October 2021 doi:10.20944/preprints202110.0406.v1

I···CH_2=C distances are in the range of 3.526-3.692 Å (Figure S1). In the XB-based azobenzene, a short distance exists between the negative equatorial region of iodine atom and carbon of the electron deficient fluorinated group (I···C2 distance = 3.652 Å). This phenomenon highlights the dual character of halogen atoms, and more particularly of iodine, that can behave both as electron donor and acceptor.[39][40] Finally, the supramolecular architecture features N-H···O hydrogen bonds (H3···O2 distance of 2.12(6) Å) involving the amide functional group. Another interesting feature concerns the layered organization of the units in a non-centrosymmetric fashion. Further studies will concern the non linear optical properties of this compound.[41][42]

2.3 Halogen bonding properties

The crystallographic study of **I-azo-NO2** and **I-azo-NH-MMA** has confirmed that the tetrafluoroiodobenzene ring is a versatile and reliable XB donor group allowing the formation of complicated architectures by self-assembly.[43]

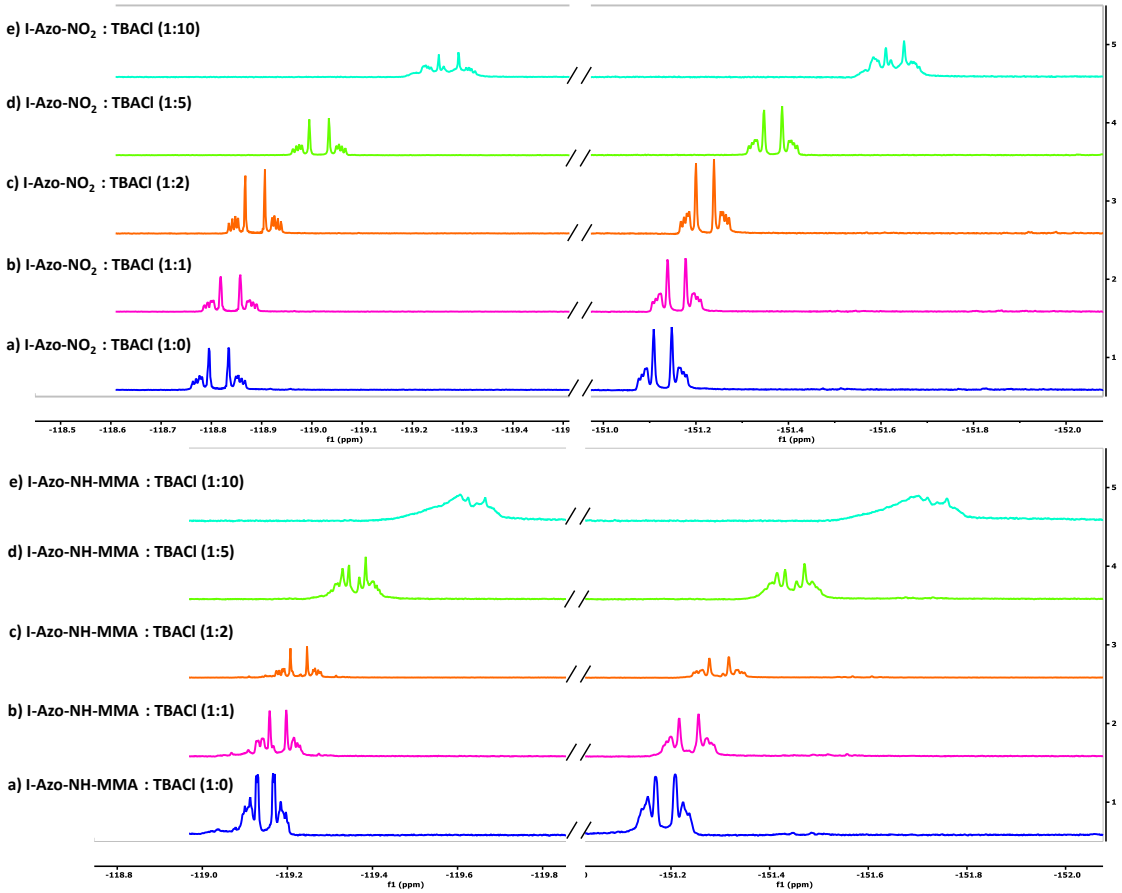

Figure 5. Stack plot of ^{19}F NMR spectra of **I-azo-NO2** and **I-azo-NH-MMA** ($CDCl_3$), at different molar ratios of **I-azo-NO2/TBACl** (top) and **I-azo-NH-MMA/TBACl** (bottom). Molar ratios: a) 1:0; b) 1:1; c) 1:2; d) 1:5; e) 1:10.

A further study aimed at highlighting the ability of the XB group to function in an intermolecular recognition process. Halide anions are particularly effective in the construction of robust supramolecular architectures, and several research works have reported the sensing of anions by halogen bonding.[44][45] Therefore, a ^{19}F NMR spectroscopic analysis was performed to monitor the interaction of the XB donor azo dyes with chloride anions in solution. In practice, **I-azo-NO2** and **I-azo-NH-MMA** were challenged with increasing quantities of tetrabutylammonium chloride (**TBACl**) in deuterated chloroform using bis(2,2,2-trifluoroethyl) ether as internal reference standard. The NMR titration experiments reveal an upfield shift of both C-F signals corresponding to fluorine

Preprints (www.preprints.org) | NOT PEER-REVIEWED | Posted: 27 October 2021 doi:10.20944/preprints202110.0406.v1

atoms *ortho* and *meta* to iodine atom upon treatment with **TBACl** (**Figure 5**). The ^{19}F NMR resonances for **I-azo-NO2** and **I-azo-NH-MMA** exhibit marked variations with δ decreasing by *ca.* -0.5 ppm in the presence of 10 equivalents of **TBACl**. Note that the same trend is observed with **I-azo-NH2** (**Figure S2**). In these cases, this shifting behavior is attributed to formation of I···Cl^- halogen bonded adducts in solution.

2.4 Photoresponsive properties

Subsequently, the photo responsiveness of these compounds was investigated. For this, dichloromethane solutions of **I-azo-NO2** and **I-azo-NH-MMA** and an acetonitrile solution of **I-azo-NH2** were treated by UV light irradiation (366 nm) (**Figure 6**). As concerns **I-azo-NO2** and **I-azo-NH-MMA**, the UV-vis spectra reveal a significant decrease of the main band at ~360 nm assigned to the $\pi \rightarrow \pi^*$ absorption, and a slight strengthening of $n \rightarrow \pi^*$ band at ~460 nm. The same trend is observed for **I-azo-NH2** but the main band is slightly shifted at 389 nm. These variations are typically observed for a conformational change of the diazobenzene unit, indicating a *trans* to *cis* isomerization. The reversible character of this phenomenon was demonstrated through a relaxation kinetic study that occurs within 8 h for all compounds after leaving the solutions in darkness or after irradiation with white light for 2 min (**Figure 6**).

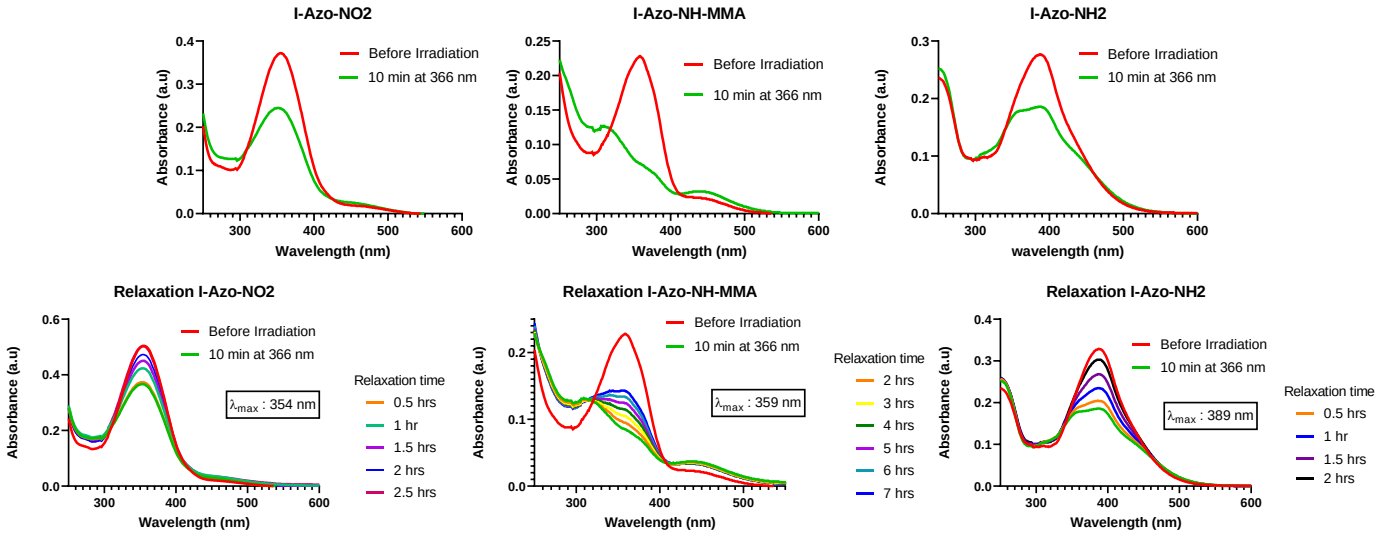

Figure 6. UV-Vis spectra for **I-azo-NO2** (top left), **I-azo-NH-MMA** (top middle) and **I-azo-NH2** (top right) before (red) and after (green) a 10 minutes exposure to 366 nm light. Thermal relaxation spectra in the dark for **I-azo-NO2** (bottom left), **I-azo-NH-MMA** (bottom middle) and **I-azo-NH2** (bottom right)

2.5 pH sensitivity

4-aminoazobenzene belongs to a family of dyes that undergo protonation accompanying a pronounced color change in acidic environment.[46] In addition to the isomerization and XB donor properties, the pH sensitivity of **I-azo-NH2** was demonstrated in solution. After solubilization in acetonitrile, the neutral medium reveals an orange color that turns red after addition of one drop of concentrated HCl 36% (**Figure 7**). Afterwards, this system exhibits a reversible color change upon addition of few drops of sodium hydroxide. **I-azo-NH2** is thereby endowed with a triple stimuli responsiveness.

Preprints (www.preprints.org) | NOT PEER-REVIEWED | Posted: 27 October 2021 doi:10.20944/preprints202110.0406.v1

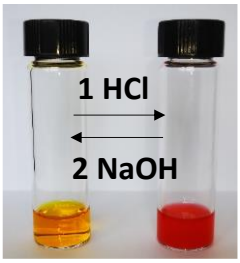

Figure 7. Acetonitrile solution of **I-azo-NH2** (left) and after acidic treatment (right).

3. Materials and Methods

All non-aqueous reactions were run in oven-dried glassware under a positive pressure of argon or nitrogen, with exclusion of moisture from reagents and glassware using standard techniques for manipulating air-sensitive compounds. Solvents were purchased from Chemlabs and dried using molecular sieves 4 Å or standard distillation technique. Iodopentafluorobenzene was purchased from Fluorochem. Nitroaniline was purchased from Apollo scientific (Nitroaniline was purified by flash chromatography on silica gel before use). Na_2S, $NaNO_2$ and Phenol were purchased from Merck. Methyl methacrylate was purchased from TCI chemicals. Reactions were monitored by analytical thin-layer chromatography (TLC) performed on pre-coated, aluminum-backed silica gel plates. Visualization of the developed chromatogram was performed by UV absorbance at 254 nm or 366 nm. Flash chromatography was performed on 230-400 mesh silica gel with the indicated solvent systems. Infrared spectra were recorded on a IRAffinity-1 Shimadzu FT-IR spectrometer and are reported in reciprocal centimeters (cm^{-1}). Routine nuclear magnetic resonance spectra were recorded on JEOL 400 Hz. Chemical shifts for ^{1}H and ^{13}C NMR spectra are recorded in parts per million from solvent resonance as the internal standard. Data are reported as follows: chemical shift, integration, multiplicity (s = singlet, d = doublet, dd = double doublet, t = triplet, q = quartet, m = multiplet and br = broad), and coupling constant in Hz. High-resolution mass spectrometry spectra were recorded on a MS QTOF-6520 Agilent for structure confirmation. UV Spectra were recorded on a Spectrophotometer Shimadzu UV-1800 in the 250 nm-600 nm range for each spectrum.

3.1 Synthetic procedures

4-((4-nitrophenyl)diazenyl)phenol (HO-azo-NO2).

This compound was prepared according to a previously reported procedure.[28]

4-Nitroaniline (3 g, 0.022 mol) was added to the hydrochloric acid aqueous solution (10%, 66 ml) and was stirred until complete dissolution. Sodium nitrite (1.95 g, 0.029 mol) was dissolved in 55 mL water and was added dropwise to the above solution within 1 h, then stirred for another 30 minutes, keeping the temperature below 0 °C. Phenol (2.66 g, 0.028 mol) and sodium hydroxide (1.11 g, 0.028 mol) were dissolved in water (40 ml), and the mixture was added dropwise to the diazonium salt solution within 1 h, keeping the temperature below 0 °C. The reaction was completed after stirring for another 3 h below 2 °C. After stirring at room temperature for 24 h, an orange product was precipitated and collected by filtration. The product was pure enough to be used without any further purification.

Yield: 96%. **Mp:** 218-220 °C.

^{1}H NMR (400 MHz, $CDCl_3$, ppm) δ 8.39 (2H, d, *J* = 9.2 Hz), 8.00 (2H, d, *J* = 9.2 Hz), 7.96 (2H, d, *J* = 8.8 Hz), 7.00 (2H, d, *J* = 8.8 Hz). **^{13}C NMR (400 MHz, $CDCl_3$, ppm)** δ, 160.42, 156.18, 148.36, 147.01, 126.02, 124.86, 123.25, 116.28.

4-((4-(2,3,5,6-tetrafluoro-4-iodophenoxy)phenyl)diazenyl)nitrobenzene (I-azo-NO2).

HO-azo-NO2 (1.0 g, 1 equiv.) was dissolved in DMF (15 mL) at 50 °C. Potassium carbonate (1.3 equiv.) was added to the reaction mixture and vigorously stirred for 20 min. Pentafluoroiodobenzene (1.1 equiv.) was added dropwise to the reaction mixture and the

Preprints (www.preprints.org) | NOT PEER-REVIEWED | Posted: 27 October 2021 doi:10.20944/preprints202110.0406.v1

reaction was stirred for 6 h, and progress of the reaction was followed by TLC (eluent: dichloromethane). Upon complete conversion of **HO-azo-NO2**, the reaction was precipitated in water and the solid was washed with *n*-hexane yielding **I-azo-NO2** as a deep red solid. Furthermore, the aqueous layer was extracted with diethyl ether three times, and the organic layer was dried over anhydrous sodium sulphate (Na_2SO_4) and concentrated to afford **I-azo-NO2.**

Yield: 95%. **Mp:** 165-168 °C.

^{1}H NMR (400 MHz, $CDCl_3$, ppm) δ 8.37 (2H, d, *J* = 9.2 Hz), 8.00 (4H, m), 7.13 (2H, d, *J* = 9.2 Hz,). **^{13}C NMR (101 MHz, $CDCl_3$, ppm)** δ 159.78, 155.79, 148.94, 148.82, 125.69, 124.89, 123.53, 116.26. **^{19}F NMR (376 MHz, $CDCl_3$, ppm)** δ -118.85, -151.16. **HR-MS (ESI) $[M-H]^+$ Calculated:** 517.9619; **Found:** 517.9618 (0.26 ppm)

4-((4-aminophenyl)diazenyl)phenol (HO-azo-NH2).

This compound was prepared according to a previously reported procedure.[28]

HO-azo-NO2 (3g, 1 equiv., 12.35 mmol) is dissolved in dioxane (50 mL) and an aqueous solution of Na_2S (3.85 g, 6 equiv., 49.4 mmol) is added to the reaction mixture at 70 °C in two times t = 0 min and t = 3 hrs. The reaction is stirred overnight and stopped once there is no more evidence of starting material by TLC. Dioxane is concentrated and the crude material is extracted three times with diethyl ether, washed with an aqueous solution of sodium carbonate, dried over sodium sulphate and the organic layer is concentrated affording a red solid. The crude material was purified by silica gel column chromatography (eluent: dichloromethane) to give **HO-azo-NH2** as a red powder.

Yield: 92%. **Mp** : 185 °C (decomposed)

^{1}H NMR (400 MHz, CD_3OD, ppm) δ 7.68 (2H, d, *J* = 8.8 Hz), 7.65 (2H, d, *J* = 8.8 Hz), 6.86 (2H, d, *J* = 8.8 Hz), 6.74 (2H, d, *J* = 8.8 Hz). **^{13}C NMR (101 MHz, CD_3OD, ppm)** δ 160.66, 152.53, 147.75, 145.86, 125.48, 124.94, 116.56, 115.37.

4-((4-(2,3,5,6-tetrafluoro-4-iodophenoxy)phenyl)diazenyl)aniline (I-azo-NH2).

HO-azo-NH2 (2.15 g, 1 equiv., 10.10 mmol) was dissolved in DMF (25 mL) at 50 °C. Potassium carbonate (1.81 g, 1.3 equiv., 13.13 mmol) was added to the reaction mixture and vigorously stirred for 20 min. Pentafluoroiodobenzene (2.97 g, 1.2 equiv., 20.2 mmol) was added dropwise to the reaction mixture and the reaction was stirred for 6 h, and progress of the reaction was followed by TLC (eluent: dichloromethane). Upon complete conversion of **HO-azo-NH2**, the reaction was precipitated in water and the solid was washed with *n*-hexane yielding **I-azo-NH2** as an orange solid. Furthermore, the aqueous layer was extracted with diethyl ether three times, and the organic layer was dried over anhydrous Na_2SO_4 and concentrated to afford **I-azo-NH2.**

Yield: 91%. **Mp:** 165-168 °C.

^{1}H NMR (400 MHz, $CDCl_3$, ppm) δ 7.85 (2H, d, *J* = 9.2 Hz), 7.78 (2H, d, *J* = 8.8 Hz), 7.06 (2H, d, *J* = 9.2 Hz), 6.73 (2H, d, *J* = 8.8 Hz), 4.05 (2H, br). **^{13}C NMR (101 MHz, $CDCl_3$, ppm)** δ 157.98, 149.72, 149.52, 145.58, 125.20, 124.22, 116.07, 114.77. **^{19}F NMR (376 MHz, $CDCl_3$, ppm)** δ -119.37, -151.23.

HR-MS (ESI) $[M+H]^+$ Calculated: 487.9877; **Found:** 487.9900 (4.54 ppm)

***N*-(4-((4-(2,3,5,6-tetrafluoro-4-iodophenoxy)phenyl)diazenyl)phenyl)methacrylamide (I-azo-NH-MMA).** To a stirred solution of **I-azo-NH2** (0.5g, 1.03 mmol, 1 equiv.) in dichloromethane (3 mL) were added triethylamine (430 µL, 3.08 mmol, 3 equiv.) and methacryloyl chloride (150 µL, 1.54 mmol, 1.5 equiv.) at 0 °C. After stirring for 5 minutes, the mixture was allowed to warm up to room temperature and stirred for 1 h. Then the reaction was quenched with H_2O and extracted with dichloromethane (3 × 15 mL). The combined organic layers were washed with brine, dried over anhydrous Na_2SO_4, concentrated under reduced pressure and purified by column chromatography using dichloromethane as eluent to afford the titled compound.

Yield: 87%. **Mp:** 200-202 °C.

Preprints (www.preprints.org) | NOT PEER-REVIEWED | Posted: 27 October 2021 doi:10.20944/preprints202110.0406.v1

^{1}H NMR (400 MHz, $CDCl_3$) δ 7.93 (2H, d, *J* = 8.8 Hz), 7.929 (2H, d, *J* = 9.2 Hz) 7.74 (2H, d, *J* = 9.2 Hz), 7.67 (s, 1H), 7.09 (2H, d, *J* = 8.8 Hz), 5.84 (1H, m), 5.52 (1H, m), 2.09 (3H, dd, *J* = 1.6 Hz, *J* = 0.9 Hz). **^{13}C NMR (101 MHz, $CDCl_3$)** δ 166.64, 149.23, 149.14, 140.97, 140.47, 124.79, 124.13, 120.41, 120.09, 116.12, 18.89. **^{19}F NMR (376 MHz, $CDCl_3$)** δ -122.92, -154.97.

HR-MS (ESI) $[M+H]^+$ Calculated: 556.0150; **Found:** 556.0149 (1.65 ppm)

3.2 X-ray crystallography

For the structure of **I-azo-NO2** and **I-azo-NH-MMA**, X-ray intensity data were collected at 100 K, on a Rigaku Oxford Diffraction Supernova Dual Source (Cu at zero) diffractometer equipped with an Atlas CCD detector using ω scans and CuKα (λ = 1.54184 Å) radiation. The images were interpreted and integrated with the program CrysAlisPro.[47] Using Olex2,[48] the structure was solved by direct methods using the ShelXT structure solution program and refined by full-matrix least-squares on F^2 using the ShelXL program package.[49][50] Non-hydrogen atoms were anisotropically refined and the hydrogen atoms in the riding mode with isotropic temperature factors fixed at 1.2 times U(eq) of the parent atoms (1.5 times for methyl groups).

3.3 ^{19}F NMR Titrations

Titrations of **I-azo-NO2**, **I-azo-NH2** and **I-azo-NH-MMA** with tetrabutylammonium chloride salt (TBACl) was monitored by ^{19}F NMR. Stock solutions of 25 mM (2 mL) and 100 mM (1 mL) of azo dyes and TBACl were prepared in $CDCl_3$. Bis(2,2,2–trifluoroethyl) ether was used as internal standard. Titration samples were prepared as follows:

Molar ratio of azo-dye:TBACl	Volume of azo-dye stock solution (μL)	Volume of TBACl stock solution (μL)	Volume of $CDCl_3$ (μL)	Total Volume (μL)
1:0	200	0	500	700
1:1	200	50	450	700
1:2	200	100	400	700
1:5	200	250	250	700
1:10	200	500	0	700

3.4 UV–Vis analysis of azobenzenes

UV-visible spectroscopic studies were performed with solutions of 10 μM of azobenzene derivatives in dichloromethane for **I-azo-NO2** and **I-azo-NH-MMA** and acetonitrile for **I-azo-NH2**. Spectra were recorded before and after irradiation at 366 nm for 10 min. The kinetics of *cis* to *trans* isomerization were determined by recording absorption spectra every 30 min for 8 hours after 10 min of irradiation at 366 nm.

3.5 pH sensitivity

3 mg of **I-azo-NH2** were solubilized in 3 ml of acetonitrile. After addition of two to three drops of HCl 36%, the solution turns red. Then, 2 drops of concentrated NaOH solution (28 M) were added, leading to an orange solution.

4. Conclusions

In summary, we reported the synthesis of new azobenzene derivatives bearing halogen bond donor groups. The X-ray analysis of **I-azo-NO2** and **I-azo-NH-MMA** highlights supramolecular arrangements developing undulating chains due to non-covalent bonds. In **I-azo-NO2**, the nitro group is simultaneously engaged in orthogonal hydrogen and halogen bonds which has been scarcely reported to date. In light of the literature, the self-complementary Ar-I···O_2N-Ar synthon can self-assemble in a head-to-tail mode, arising

thus as a very appealing motif to design supramolecular architectures in a high reliability. As concerns **I-azo-NH-MMA**, a non-centrosymmetric organization was observed thanks to uncommon I···CH_2=C halogen bonding. A survey of the Cambridge Structural Database reveals that only four structures involve this contact. In addition to the crystallographic studies, ^{19}F NMR spectroscopic analyses have emphasized that such compounds can be involved in intermolecular recognition processes, as proposed through I···Cl^- halogen bonding in solution. Subsequently, the photo responsiveness of all XB-based compounds was studied by irradiation at 366 nm. As expected, a *trans* to *cis* isomerization was confirmed by UV-vis analysis, this phenomenon being reversible. Finally, the synthetic intermediate **I-azo-NH2** shows a light and pH responsive profile in combination with a halogen bond donor ability, with a potential application for anion sensing. Further works will aim at preparing polymeric materials using these stimuli responsive units and their application in the preparation of functional compounds.

Supplementary Materials: The following are available online at www.mdpi.com/xxx/s1, Figure S1: X-ray structures of HOQKAC (top left), HOTZOH (top right), PEQVOZ (bottom left) and USAJIK (bottom right) showing the I···CH_2=C halogen bonds found in the Cambridge Structural Database (CSD version 5.42 updates, Sep 2021). Colors are as follows: grey, C; blue, N; red, oxygen; white, H; orange, S; purple, I. Figure S2: Stack plot of ^{19}F NMR spectra of **I-azo-NH2** ($CDCl_3$), at different molar ratios of **I-azo-NH2**/**TBACl**. Molar ratios: a) 1:0; b) 1:1; c) 1:2; d) 1:5; e) 1:10.

Author Contributions: Conceptualization, F.M.; methodology, F.M., P.F and S.K.; software, K.V.H.; validation, F.M., P.F, M.G. and S.K.; formal analysis, F.M., P.F, S.K., M.G. and K.V.H.; investigation, F.M., P.F. and S.K.; resources, F.M.; data curation, P.F., S.K. and K.V.H.; writing—original draft preparation, F.M., P.F and S.K.; writing—review and editing, F.M.; supervision, F.M.; project administration, F.M.; funding acquisition, F.M. All authors have read and agreed to the published version of the manuscript.

Funding: S.K. and F.M. thank ULB for the financial support (PDR 35275398).

Data Availability Statement: In this section, please provide details regarding where data supporting reported results can be found, including links to publicly archived datasets analyzed or generated during the study. Please refer to suggested Data Availability Statements in section "MDPI Research Data Policies" at https://www.mdpi.com/ethics. You might choose to exclude this statement if the study did not report any data.

Acknowledgments: We are also grateful to the analytical platform of the faculty of pharmacy (ULB) for mass spectroscopy analyses.

Conflicts of Interest: "The authors declare no conflict of interest."

References

1. Zhang, X.; Chen, L.; Lim, K.H.; Gonuguntla, S.; Lim, K.W.; Pranantyo, D.; Yong, W.P.; Yam, W.J.T.; Low, Z.; Teo, W.J.; et al. The Pathway to Intelligence Using Stimuli-Responsive Materials as Building Blocks for Constructing Smart and Functional Systems. *Adv. Mater.* **2019**, *31*, 1804540, doi:10.1002/adma.201804540.
2. McCune, J.A.; Mommer, S.; Parkins, C.C.; Scherman, O.A. Design Principles for Aqueous Interactive Materials: Lessons from Small Molecules and Stimuli-Responsive Systems. *Adv. Mater.* **2020**, *32*, 1906890, doi:10.1002/adma.201906890.
3. Mrinalini, M.; Prasanthkumar, S. Recent Advances on Stimuli-Responsive Smart Materials and Their Applications. *Chempluschem* **2019**, *84*, 1103–1121, doi:10.1002/cplu.201900365.
4. Rahim, M.A.; Jan, N.; Khan, S.; Shah, H.; Madni, A.; Khan, A.; Jabar, A.; Khan, S.; Elhissi, A.; Hussain, Z.; et al. Recent Advancements in Stimuli Responsive Drug Delivery Platforms for Active and Passive Cancer Targeting. *Cancers (Basel).* **2021**, *13*, 1–52, doi:10.3390/cancers13040670.
5. Hu, L.; Shu, T.; Wan, Y.; Fang, C.; Gao, F.; Serpe, M.J. Recent Advances in Stimuli-Responsive Polymers for Sensing and Actuation. *Mol. Syst. Des. Eng.* **2021**, *6*, 108–121, doi:10.1039/d0me00133c.
6. Gu, X.; Wang, J.; Liu, X.; Zhao, D.; Wang, Y.; Gao, H.; Wu, G. Temperature-Responsive Drug Delivery Systems Based on

Polyaspartamides with Isopropylamine Pendant Groups. *Soft Matter* **2013**, *9*, 7267–7273, doi:10.1039/c3sm50904d.

7. Suedee, R.; Jantarat, C.; Lindner, W.; Viernstein, H.; Songkro, S.; Srichana, T. Development of a PH-Responsive Drug Delivery System for Enantioselective-Controlled Delivery of Racemic Drugs. *J. Control. Release* **2010**, *142*, 122–131, doi:10.1016/j.jconrel.2009.10.011.
8. Maggini, L.; Raquez, J.-M.; Marega, R.; Jensen Ahrens, J.; Pineux, F.; Meyer, F.; Dubois, P.; Bonifazi, D. Magnetic Poly(Vinylpyridine)-Coated Carbon Nanotubes: An Efficient Supramolecular Tool for Wastewater Purification. *ChemSusChem* **2013**, *6*, 367 – 373, doi:10.1002/cssc.201200413.
9. Wang, Y.; Liu, D.; Zheng, Q.; Zhao, Q.; Zhang, H.; Ma, Y.; Fallon, J.K.; Fu, Q.; Haynes, M.T.; Lin, G.; et al. Disulfide Bond Bridge Insertion Turns Hydrophobic Anticancer Prodrugs into Self-Assembled Nanomedicines. *Nano Lett.* **2014**, *14*, 5577–5583, doi:10.1021/nl502044x.
10. Zhou, Y.-N.; Li, J.-J.; Zhang, Q.; Luo, Z.-H. Light-Responsive Smart Surface with Controllable Wettability and Excellent Stability. *Langmuir* **2014**, *30*, 12236–12242, doi:org/10.1021/la501907w.
11. Tao, Y.; Chan, H.F.; Shi, B.; Li, M.; Leong, K.W. Light: A Magical Tool for Controlled Drug Delivery. *Adv. Funct. Mater.* **2020**, *30*, 1–28, doi:10.1002/adfm.202005029.
12. Giles, L.W.; Faul, C.F.J.; Tabor, R.F. Azobenzene Isomerization in Condensed Matter: Lessons for the Design of Efficient Light-Responsive Soft-Matter Systems. *Mater. Adv.* **2021**, *2*, 4152–4164, doi:10.1039/d1ma00340b.
13. Merino, E. Synthesis of Azobenzenes: The Coloured Pieces of Molecular Materials. *Chem. Soc. Rev.* **2011**, *40*, 3835–3853, doi:10.1039/c0cs00183j.
14. Bandara, H.M.D.; Burdette, S.C. Photoisomerization in Different Classes of Azobenzene. *Chem. Soc. Rev.* **2012**, *41*, 1809–1825, doi:10.1039/c1cs15179g.
15. Dong, M.; Babalhavaeji, A.; Samanta, S.; Beharry, A.A.; Woolley, G.A. Red-Shifting Azobenzene Photoswitches for in Vivo Use. *Acc. Chem. Res.* **2015**, *48*, 2662–2670, doi:10.1021/acs.accounts.5b00270.
16. Cavallo, G.; Metrangolo, P.; Milani, R.; Pilati, T.; Priimagi, A.; Resnati, G.; Terraneo, G. The Halogen Bond. *Chem. Rev.* **2016**, *116*, 2478–2601, doi:10.1021/acs.chemrev.5b00484.
17. Gilday, L.C.; Robinson, S.W.; Barendt, T.A.; Langton, M.J.; Mullaney, B.R.; Beer, P.D. Halogen Bonding in Supramolecular Chemistry. *Chem. Rev.* **2015**, *115*, 7118–7195, doi:10.1021/cr500674c.
18. Bulfield, D.; Huber, S.M. Halogen Bonding in Organic Synthesis and Organocatalysis. *Chem. - A Eur. J.* **2016**, *22*, 14434–14450, doi:10.1002/chem.201601844.
19. Wilcken, R.; Zimmermann, M.O.; Lange, A.; Joerger, A.C.; Boeckler, F.M. Principles and Applications of Halogen Bonding in Medicinal Chemistry and Chemical Biology. *J. Med. Chem.* **2013**, *56*, 1363–1388, doi:10.1021/jm3012068.
20. Berger, G.; Frangville, P.; Meyer, F. Halogen Bonding for Molecular Recognition : New Developments in Materials and Biological Sciences. *Chem. Commun.* **2020**, *56*, 4970–4981, doi:10.1039/D0CC00841A.
21. Priimagi, A.; Cavallo, G.; Forni, A.; Gorynsztejn-Leben, M.; Kaivola, M.; Metrangolo, P.; Milani, R.; Shishido, A.; Pilati, T.; Resnati, G.; et al. Halogen Bonding versus Hydrogen Bonding in Driving Self-Assembly and Performance of Light-Responsive Supramolecular Polymers. *Adv. Funct. Mater.* **2012**, *22*, 2572–2579, doi:10.1002/adfm.201200135.
22. Saccone, M.; Dichiarante, V.; Forni, A.; Goulet-Hanssens, A.; Cavallo, G.; Vapaavuori, J.; Terraneo, G.; Barrett, C.J.; Resnati, G.; Metrangolo, P.; et al. Supramolecular Hierarchy among Halogen and Hydrogen Bond Donors in Light-Induced Surface Patterning. *J. Mater. Chem. C* **2015**, *3*, 759–768, doi:10.1039/C4TC02315C.
23. Bushuyev, O.S.; Corkery, T.C.; Barrett, C.J.; Friščić, T. Photo-Mechanical Azobenzene Cocrystals and in Situ X-Ray Diffraction Monitoring of Their Optically-Induced Crystal-to-Crystal Isomerisation. *Chem. Sci.* **2014**, *5*, 3158, doi:10.1039/c4sc00987h.
24. Tong, X.; Qiu, Y.; Zhao, X.; Xiong, B.; Liao, R.; Peng, H.; Liao, Y.; Xie, X. Visible Light-Triggered Gel-to-Sol Transition in Halogen-Bond-Based Supramolecules. *Soft Matter* **2019**, *15*, 6411–6417, doi:10.1039/c9sm01310e.
25. Saccone, M.; Cavallo, G.; Metrangolo, P.; Resnati, G.; Priimagi, A. Halogen-Bonded Photoresponsive Materials. *Top. Curr. Chem.* **2015**, *359*, 147–166, doi:10.1007/128_2014_615.

26. Berger, G.; Soubhye, J.; Meyer, F. Halogen Bonding in Polymer Science: From Crystal Engineering to Functional Supramolecular Polymers and Materials. *Polym. Chem.* **2015**, *6*, 3559–3580, doi:10.1039/C5PY00354G.
27. Chikh Alard, I.; Soubhye, J.; Berger, G.; Gelbcke, M.; Spassov, S.; K. Amighi; Goole, J.; Meyer, F. Triple-Stimuli Responsive Polymers with Fine Tuneable Magnetic Responses. *Polym. Chem.* **2017**, *8*, 2450–2456, doi:10.1039/c7py00218a.
28. Zhou, D.; Wang, Y.; Jia, J.; Yu, W.; Qu, B.; Li, X.; Sun, X. H-Bonding and Charging Mediated Aggregation and Emission for Fluorescence Turn-on Detection of Hydrazine Hydrate. *Chem. Commun.* **2015**, *51*, 10656–10659, doi:org/10.1039/C5CC02897C.
29. Tothadi, S.; Desiraju, G.R. Designing Ternary Cocrystals with Hydrogen Bonds and Halogen Bonds. *Chem. Commun.* **2013**, *49*, 7791–7793, doi:10.1039/c3cc43822h.
30. Batsanov, S.S. Van Der Waals Radii of Elements. *Inorg. Chem.* **2001**, *37*, 1031–1046, doi:10.1023/A.
31. Voth, A.R.; Khuu, P.; Oishi, K.; Ho, P.S. Halogen Bonds as Orthogonal Molecular Interactions to Hydrogen Bonds. *Nat. Chem.* **2009**, *1*, 74–79, doi:10.1038/NCHEM.112.
32. Vasylyeva, V.; Nayak, S.K.; Terraneo, G.; Cavallo, G.; Metrangolo, P.; Resnati, G. Orthogonal Halogen and Hydrogen Bonds Involving a Peptide Bond Model. *CrystEngComm* **2014**, *16*, 8102–8105, doi:10.1039/c4ce01514b.
33. Terwingen, S. van; Brüx, D.; Wang, R.; Englert, U. Hydrogen-Bonded and Halogen-Bonded Orthogonal Interactions for the Chloride Anion of a Pyrazolium Salt. *Molecules* **2021**, *26*, 3982, doi:org/10.3390/molecules26133982.
34. Thalladi, V.R.; Goud, B.S.; Hoy, V.J.; Allen, F.H.; Howard, J.A.K.; Desiraju, G.R. Supramolecular Synthons in Crystal Engineering. Structure Simplification, Synthon Robustness and Supramolecular Retrosynthesis. *Chem. Commun.* **1996**, 401–402, doi:10.1039/cc9960000401.
35. Lu, S.; Ng, S.V.H.; Lovato, K.; Ong, J.Y.; Poh, S.B.; Ng, X.Q.; Kürti, L.; Zhao, Y. Practical Access to Axially Chiral Sulfonamides and Biaryl Amino Phenols via Organocatalytic Atroposelective N-Alkylation. *Nat. Commun.* **2019**, *10*, 3061, doi:10.1038/s41467-019-10940-4.
36. Shao, W.H.; Chen, B.Y.; Cheng, X.R.; Yuan, H.; Chen, H.; Chang, W.L.; Ye, J.; Lin, S.; Sun, Q.Y.; Zhang, W.D. Synthesis and Evaluation of New α-Methylene-γ-Lactone Carbamates with NO Production Inhibitory Effects in Lipopolysaccharide-Induced RAW 264.7 Macrophages. *Eur. J. Med. Chem.* **2015**, *93*, 274–280, doi:10.1016/j.ejmech.2015.02.016.
37. Röse, P.; Emge, S.; Yoshida, J.I.; Hilt, G. Electrochemical Selenium- and Iodonium-Initiated Cyclisation of Hydroxy-Functionalised 1,4-Dienes. *Beilstein J. Org. Chem.* **2015**, *11*, 174–183, doi:10.3762/bjoc.11.18.
38. Ren, X.; Tang, L.; Shen, C.; Li, H.; Wang, P.; Dong, K. Enantioselective Hydroesterificative Cyclization of 1,6-Enynes to Chiral γ-Lactams Bearing a Quaternary Carbon Stereocenter. *Org. Lett.* **2021**, *23*, 3561–3566, doi:10.1021/acs.orglett.1c00952.
39. Berger, G.; Soubhye, J.; van der Lee, A.; Vande Velde, C.; Wintjens, R.; Dubois, P.; Clément, S.; Meyer, F. Interplay between Halogen Bonding and Lone Pair-π Interactions: A Computational and Crystal Packing Study. *Chempluschem* **2014**, *79*, 552–558, doi:10.1002/cplu.201400005.
40. Berger, G.; Robeyns, K.; Soubhye, J.; Wintjens, R.; Meyer, F. Halogen Bonding in a Multi-Connected 1,2,2-Triiodo-Alkene Involving Geminal and/or Vicinal Iodines: A Crystallographic and DFT Study. *CrystEngComm* **2016**, *18*, doi:10.1039/c5ce02230d.
41. Cariati, E.; Forni, A.; Biella, S.; Metrangolo, P.; Meyer, F.; Resnati, G.; Righetto, S.; Tordin, E.; Ugo, R. Tuning Second-Order NLO Responses through Halogen Bonding. *Chem. Commun.* **2007**, 2590–2592, doi:10.1039/b702724a.
42. Virkki, M.; Tuominen, O.; Forni, A.; Saccone, M.; Metrangolo, P.; Resnati, G.; Kauranen, M.; Priimagi, A. Halogen Bonding Enhances Nonlinear Optical Response in Poled Supramolecular Polymers. *J. Mater. Chem. C* **2015**, *3*, 3003–3006, doi:10.1039/c5tc00484e.
43. Baldrighi, M.; Metrangolo, P.; Meyer, F.; Pilati, T.; Proserpio, D.; Resnati, G.; Terraneo, G. Halogen-Bonded and Interpenetrated Networks through the Self-Assembly of Diiodoperfluoroarene and Tetrapyridyl Tectons. *J. Fluor. Chem.* **2010**, *131*, 1218–1224, doi:10.1016/j.jfluchem.2010.06.001.
44. Kumar, V.; Pilati, T.; Terraneo, G.; Meyer, F.; Metrangolo, P.; Resnati, G. Halogen Bonded Borromean Networks by Design : Topology Invariance and Metric Tuning in a Library of Multi-Component Systems. *Chem. Sci.* **2017**, *8*, 1801–1810,

doi:10.1039/C6SC04478F.

45. Lim, J.Y.C.; Beer, P.D. Sigma-Hole Interactions in Anion Recognition. *Chem* **2018**, *4*, 731–783, doi:10.1016/j.chempr.2018.02.022.
46. Machida, K.; Kim, B.-K.; Saito, Y.; Igarashi, K.; Uno, T. Resonance Raman Spectra of Acid-Base Indicators. I. p - Aminoazobenzene Derivatives. *Bull. Chem. Soc. Jpn.* **1974**, *47*, 78–83, doi:10.1246/bcsj.47.78.
47. Rigaku Oxford Diffraction, (2019), CrysAlisPro Software Systems, Rigaku Corporation, Oxford, UK.
48. Dolomanov, O. V.; Bourhis, L.J.; Gildea, R.J.; Howard, J.A.K.; Puschmann, H. OLEX2: A Complete Structure Solution, Refinement and Analysis Program. *J. Appl. Crystallogr.* **2009**, *42*, 339–341, doi:10.1107/S0021889808042726.
49. Sheldrick, G.M. SHELXT - Integrated Space-Group and Crystal-Structure Determination. *Acta Crystallogr. Sect. A Found. Crystallogr.* **2015**, *71*, 3–8, doi:10.1107/S2053273314026370.
50. Sheldrick, G.M. Crystal Structure Refinement with SHELXL. *Acta Crystallogr. Sect. C Struct. Chem.* **2015**, *71*, 3–8, doi:10.1107/S2053229614024218.